JOURNAL OF AGRICULTURAL AND FOOD CHEMISTRY

Antiatherosclerotic Effects of *Artemisia princeps* Pampanini cv. Sajabal in LDL Receptor Deficient Mice

JONG-MIN HAN,[†] MIN-JUNG KIM,[†] SEUNG-HWA BAEK,[†] SOJIN AN,[†] YUE-YAN JIN,[†] HAE-GON CHUNG,[‡] NAM-IN BAEK,[§] MYUNG-SOOK CHOI,[⊥] KYUNG-TAE LEE,[Π] AND TAE-SOOK JEONG*,[†]

National Research Laboratory of Lipid Metabolism & Atherosclerosis, KRIBB, Daejeon 305-806, Korea, Ganghwa Agricultural R&D Center, Inchon 417-830, Korea, Graduate School of Biotechnology and Plant Metabolism Research Center, Kyung-Hee University, Suwon 449-701, Korea, Department of Food Science and Nutrition, Kyungpook National University, Daegu 702-701, Korea, and College of Pharmacy, Kyung-Hee University, Seoul 130-701, Korea

Antiatherosclerotic effects of ethanolic extracts of *Artemisia princeps* Pampanini cv. Sajabal (ESJ) were investigated in low-density lipoprotein receptor deficient ($LDLR^{-/-}$) mice. The Western diet-induced high levels of total cholesterol and triglyceride were similar in the ESJ and control groups. However, circulating oxidized LDL was significantly decreased in the ESJ group ($p < 0.05$). ESJ also markedly decreased aortic expression levels of intercellular adhesion molecule-1 (ICAM-1), vascular cell adhesion molecule-1 (VCAM-1), tumor necrosis factor-α (TNF-α), and interleukin-1β (IL-1β), and reduced the aortic lesion formation and macrophage accumulation by 36.7% ($p < 0.05$) and 43% ($p < 0.01$) in the control group, respectively. Additionally, ESJ inhibited atherogenic properties with cytokine-induced surface expression of cell adhesion molecules, chemokines, and monocyte adhesion to the human umbilical vein endothelial cells (HUVECs), and simultaneously suppressed nuclear factor-κB (NF-κB) activation. These results suggest that ethanolic extracts of *Artemisia princeps* Pampanini cv. Sajabal contributes to the antiatherosclerotic and anti-inflammatory activities in $LDLR^{-/-}$ mice.

KEYWORDS: ***Artemisia princeps*** Pamp. cv; Sajabal; atherosclerosis; inflammation; oxidized LDL; NF-κB

INTRODUCTION

Oxidation of low-density lipoproteins (LDLs) is a key step in the early stages of atherosclerosis (*1*). Several lines of evidence support the existence of in vivo oxidized LDL (ox-LDL) during the development of early fatty streaks and more advanced atherosclerotic lesions (*2, 3*). Elevated blood level LDLs are trapped in the subendothelial space of the artery and cause endothelial cells and macrophages to secrete numerous cytokines that promote the entry of circulating monocytes and leukocytes into the arterial subendothelial space. Monocytes differentiate into macrophages, which rapidly engulf oxidized and aggregated LDLs using the scavenger receptors SRA, CD36, and CD68 (*3, 4*). These lead to the lipid peroxidation and facilitate cholesterol ester accumulation, which leads to the formation of foam cells with multiple cytoplasmic cholesterol ester lipid droplets (*3*).

Monocyte and leukocyte entry into the arterial subendothelial space is mediated by adhesion molecules and chemotactic factors (*5*). Adhesion molecules such as intercellular adhesion molecule-1 (ICAM-1) and vascular cell adhesion molecule-1 (VCAM-1) initiate early atherosclerotic plaque formation by promoting monocyte adhesion to endothelial cells and increasing vascular inflammation (*4, 6*).

Studies have suggested that nuclear factor-κB (NF-κB) is an obligatory mediator of the inflammatory response that activates genes encoding adhesion molecules (*7*). NF-κB is a member of the Rel family of eukaryotic transcription factors, which are involved in the regulation of immune and inflammatory processes, including cell proliferation, survival, and cellular stress responses (*8*). Mammalian NF-κB/Rel consists of homodimers and heterodimers of different subunits, including p50, p52, p65 (RelA), c-Rel, RelB, and NF-κB/Rel binding sites, which were identified upstream of the ICAM-1 and E-selectin gene transcription start sites (*9*).

Artemisia princeps Pamp. is a herbaceous plant that is widely used in Korean, Chinese, and Japanese traditional medicine for

* To whom corresponding should be addressed. Tel: +82-42-860-4558. Fax: +82-42-861-2675. E-mail: tsjeong@kribb.re.kr.
[†] KRIBB.
[‡] Ganghwa Agricultural R&D Center.
[§] Graduate School of Biotechnology and Plant Metabolism Research Center, Kyung-Hee University.
[⊥] Kyungpook National University.
[Π] College of Pharmacy, Kyung-Hee University.

10.1021/jf802639y CCC: $40.75 © 2009 American Chemical Society
Published on Web 01/23/2009

the treatment of multiple disorders including colic, vomiting, diarrhea, and irregular uterine bleeding (*10*). The use of this material as food or food constituent is well described in Wikipedia, The Free Encyclopedia (http://www.wikipedia.org). In China, it is known as huang hua ai; in Japan it is called yomogi, and the leaves are added to soups or rice; in Korea, it is called ssuk or tarae ssuk, which is widely used in Korean cuisine. It is used for making rice cake, Korean style pancake, kimch, soup, and so forth. The extracts of *A. princeps* Pamp. leaves have various aroma chemicals (*11*). *Artemisia princeps* Pamp. cv. Sajabal (SJ) is a variant cultivated in Ganghwa County, a place located in the west coast of Korea. Studies have reported that the ethanolic extracts (ESJ) possess antidiabetic and antiallergic activities (*12*, *13*). ESJ contain particularly high contents of eupatilin (204.6 mg/100 g of leaves) and jaceosidin (104.6 mg/100 g of leaves) as compared with *Artemisia* herbs from other regions (*12*, *14*). These flavonoids may play important roles in antioxidant and anti-inflammatory activities (*15*−*17*). There has been minimal evaluation of the antiatherosclerotic activities of ESJ. Therefore, we investigated the antiatherosclerotic effects of ESJ in LDLR$^{-/-}$ mice and identified potential mechanisms to inhibit early atherosclerosis, including the expression of adhesion molecules and inflammatory factors.

MATERIALS AND METHODS

Animals and Treatment. Homozygous LDL receptor deficient (LDLR$^{-/-}$, C57BL/6J background) mice were purchased from The Jackson Laboratory (Bar Harbor, ME) and housed at the Korean Research Institute of Bioscience and Biotechnology (KRIBB). Ten-week-old male LDLR$^{-/-}$ mice ($n = 20$) were randomly divided into two groups. The control group was fed a Western diet of 0.15% cholesterol and 21% fat by weight with no cholic acid (Dyets Inc., PA), while the ESJ experimental group was fed a Western diet supplemented with 1 wt %/wt diet ESJ for 8 weeks. Additionally, we used chow diet-fed C57BL/6J mice ($n = 6$, CD group) as a negative control. Mice were treated in accordance with the KRIBB Guide for the Care and Use of Laboratory Animals.

Plasma Biomarker Analysis. Total plasma lipoproteins and triglycerides were measured using an automatic blood chemical analyzer (CIBA Corning, Medfield, MA). Circulating oxidized LDLs were measured with the Mercodia Oxidized LDL ELISA kit, which determines the aldehyde modification of apolipoprotein B lysine residues. Pro-inflammatory cytokines and apolipoprotein levels were confirmed by Western blot analysis.

Preparation of Histological Sections and Measurement of Fatty Streak Lesion Area. All samples were embedded in a Tissue-Tek OCT compound (Sakura Finetek, Inc., Torrance, CA) and were placed on a cryotome model AS620 (Shandon, Pittsburgh, PA). Cryostat sections of aortic roots (10 μm) were collected and stained with oil red O. Macrophage infiltration was detected with MOMA-2, a mouse macrophage specific antibody (Serotec Inc., Raleigh, NC). Aortic sections were incubated with MOMA-2 at a 1:10 dilution overnight at 4 °C and then incubated with a FITC-conjugated rabbit antirat IgG at a 1:300 dilution for 1 h at room temperature. Aortic images were captured with a BX61 microscope (Olympus, JAPAN), and atherosclerotic lesions and MOMA-2 immunoreactivity were quantified by computer image analysis using Metamorph imaging software (Molecular devices, Japan). The proportional ratio of MOMA-2-stained areas to oil red O-stained areas was expressed as a percentage.

Reagents and Cell Culture. 2′,7′-Bis-(2-carboxyethyl)-5-(and-6)-carboxyfluorescein acetoxymethyl ester (BCECF-AM) was obtained from the Sigma Chemical Co. (St. Louis, MO), and FITC-conjugated mAbs for ICAM and VCAM-1 were provided by R&D Systems Incorporated (Minneapolis, MN). Recombinant human TNF-α was provided by Strathmann Biotech (Hannover, Germany), and anti-NF-κB p65, anti-IκBα, and most other Abs were obtained from Santa Cruz Biotechnology Incorporated (Santa Cruz, CA). Human umbilical vein endothelial cells (HUVECs) were obtained from Clonetics (San Diego, CA) and cultured in the endothelial cell basal medium-2 (EBM-2) Bullet kit (Lonza Bioscience, Verviers, Belgium).

Table 1. Effects of ESJ on Lipid Profiles of Plasma in Western Diet-Fed LDLR$^{-/-}$ Mice[a]

groups ($n = 10$)	plasma lipids (mg/dL)			
	TC	HDL-C	HDL-C/ TC	TG
CD	107 ± 19.3	63.0 ± 6.9	0.596 ± 0.049	83.2 ± 13.7
control	1223.8 ± 332.1#	83.8 ± 11.3#	0.075 ± 0.020#	664.9 ± 228.5#
ESJ	1310.8 ± 216.9	81.4 ± 5.5	0.065 ± 0.017	677.8 ± 98.8

[a] TC, total cholesterol; HDL-C, high-density lipoprotein cholesterol; TG, triglyceride. All values are expressed as mean ± S.D. #, $p < 0.05$ vs CD. CD, chow diet-fed group; control, Western diet-fed group; ESJ, 1% (wt/wt diet) ESJ supplemented Western diet-fed group.

Adhesion Assay. THP-1 cells in culture media were labeled with the BCECF-AM fluorescent dye at a 10 μM concentration at 37 °C for 1 h. The THP-1 cell distribution image was obtained with an ECLIPSE 2000 fluorescent microscope (NIKON, Japan), and fluorescence intensity was measured on a Wallac 1420 spectrofluorometer (Perkin-Elmer, Turku, Finland) from the top reading ($Ex = 488$ nm, $Em = 535$ nm).

Determination of Adhesion Molecule Expression. Cell-surface VCAM-1 and ICAM-1 expression on HUVECs was detected using a cell ELISA as described (*18*). Cells were incubated with FITC-conjugated anti-VCAM-1 and anti-ICAM-1 monoclonal antibodies. Expression of VCAM-1 and ICAM-1 was measured with a spectrofluorometer from the top reading ($Ex = 488$ nm, $Em = 535$ nm) without cell disruption and the cell distribution image obtained with an ECLIPSE 2000 fluorescent microscope.

Real-Time Quantitative RT-PCR. Total RNA was extracted from HUVECs using easy-BLUE (iNtRON Biotechnology, Korea), and cDNA was synthesized using oligo (dT) primers using Omniscript (Qiagen, Santa Clarita, CA) according to the manufacturer's instructions. PCR amplifications were quantified using the SYBRGreen PCR Master Mix (Applied Biosystems, Foster City, CA) for gene expression of VCAM-1 (NM_001078), ICAM-1 (NM_000201), CCL2/MCP-1 (NM_002982), CX3CL1/Fractalkine (NM_002996), CCL5/RANTES (NM_002985), and β-Actin (NM_001101). The following primers were used to amplify VCAM-1, ICAM-1, MCP-1, CX3CL1, CXCL8, and β-Actin: VCAM-1, 5′-ACTGTTTATTACAGCCCCGC-3′ (sense) and 5′-ACTTCAACGATGGGGACTTG-3′ (antisense); ICAM-1, 5′-GTCGAAGGTGGTTCTTCTGAGC-3′ (sense) and 5′-TCCGTCTGCAGGTCATCTTAGG-3′ (antisense); MCP-1, 5′-CTCAGCCAGATGCAATCAA-3′ (sense) and 5′-CTTGGCCACAATGGTCTTGA-3′ (antisense); CX3CL1, 5′-TCACGTGCAGCAAGATGACA-3′ (sense) and 5′-TCCTTGACCCATTGCTCCTT-3′ (antisense); CCL5, 5′-CGGGAGTACATCAACTCTTTGGA-3′ (sense) and 5′-CAAGCTAGGACAAGAGCAAGCA-3′ (antisense); β-Actin, 5′-GGCACCACACCTTCTACAAT-3′ (sense) and 5′-TCTGGGCATCCTTCACAGCT-3′ (antisense).

Western Blot Analysis. Mouse aortic tissue extracts (ABCA1, ACAT1, CYP family, scavenger receptors, adhesion molecules, and inflammatory factors), total cell extracts (ICAM-1, VCAM-1, MCP-1, CX3CL1, and IL-1β), cytoplasmic extracts (IκBα, and nuclear extracts (NF-κB p65) were fractionated by electrophoresis on 10% SDS−PAGE gels and transferred onto nitrocellulose membranes. Membranes were blotted with specific antibodies to each protein, and the peroxidases bound to the blots were detected with the ECL Western blot kit (Elpis Biotech, Korea).

Immunocytochemistry and Electrophoretic Mobility Shift Assay (EMSA). NF-κB activation was measured by assessing the p65 NF-κB subunit distribution between the cytoplasms and nuclei of HUVECs by immunofluorescence images. Briefly, confluent HUVECs were cultured on cover slides and treated with the test substances. Cells were fixed with 1% paraformaldehyde and stained with the anti-p65 primary antibody and with the Texas red-linked secondary antibody. Fluorescence photographs were obtained with BX-61 fluorescence microscopy

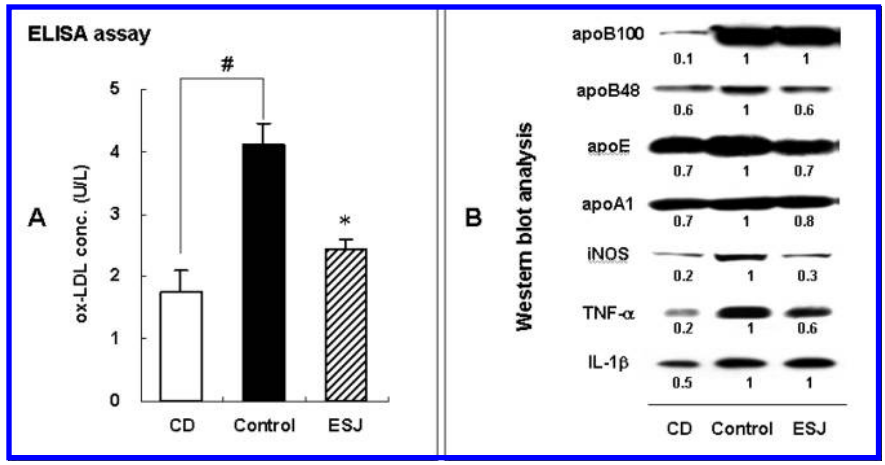

Figure 1. Effects of ESJ on circulating ox-LDL, lipoprotein levels, and inflammatory cytokines in the plasma of Western diet-fed LDLR$^{-/-}$ mice for 8 weeks. The plasmas of each group were pooled and used for protein extraction. (**A**) The level of circulating ox-LDL was quantified with a commercially available ELISA assay kit. Results are shown as the mean ± SD ($n = 3$). $^{\#}p < 0.01$ vs CD group and $^{*}p < 0.01$ vs control group. (**B**) Protein levels were analyzed by Western blot analysis. The intensity of the detected bands was quantified with a Calibrated Densitometer GS800 (Bio-Rad) with Quantity One software (version 4.4.0). CD, chow diet-fed group; Control, Western diet-fed group; ESJ, 1% (wt/wt diet) ESJ supplemented Western diet-fed group.

(Olympus, Japan). Nuclear extract preparation and EMSA conditions were described (*18*). Nuclear proteins were quantified by the Bradford method at 595 nm. EMSA was performed according to the manufacturer's instructions (Promega) with ^{32}P-labeled double stranded oligonucleotides with consensus recognition sequences for NF-κB (5′-AGTTGAGGGGACTTTCCCAGGC-3′) and Oct-1 (5′-TGTCGAATGCAAATCACTAGAA-3′).

Data Analysis. Data were expressed as mean ± SD values. Statistical significance ($p < 0.05$) between the two groups was determined from two parallel experiments with the Student's *t*-test.

RESULTS

Body weights and food intake were not significantly different between control and ESJ groups during the study period (data not shown). Large increases in total cholesterol (TC), triglycerides (TG), and LDL cholesterol were observed in plasma after 8 weeks of the Western diet. TC and TG levels were similar in the ESJ and control groups (**Table 1**).

The circulating ox-LDL levels in plasma were significantly higher in the Western diet-fed control group than in the chow diet-fed CD group ($p < 0.01$). Plasma lipids were similar in the ESJ and control groups (**Table 1**), but circulating ox-LDLs were significantly lower in the ESJ group (**Figure 1A**), suggesting that plasma lipid oxidation was decreased in the ESJ group. We determined plasma lipoprotein and cytokine levels by Western blot analysis as shown in **Figure 1B**. Each lipoprotein level showed tendency similar to that described above for lipid profiles (**Table 1**). However, circulating plasma pro-inflammatory iNOS and TNF-α levels were decreased in the ESJ group.

Atherosclerotic lesions in Western diet fed-LDLR$^{-/-}$ mice had positive oil red O staining noted in an examination of tissue cross-sections (**Figure 2A**). The mean oil red O-stained lesional area was (76.9 ± 51) × 10^3 μm^2 in the ESJ group ($p < 0.05$) and (114.8 ± 41) × 10^3 μm^2 in the control group. A 36.7% inhibition effect on ESJ group lesion formation was noted when stained areas were divided by lesion size for the entire aortic sinus (**Table 2**). Aortic sinus sections were immunostained with MOMA-2 to evaluate monocyte recruitment into the arterial wall. The MOMA-2-positive areas observed in subendothelial surfaces of the control group was 81.5 ± 15.6% and of the ESJ group was 47.5 ± 24.7% ($p < 0.01$) of the total area (**Table 2** and **Figure 2B**). VCAM-1, ICAM-1, and LOX-1 expression in the aortas from the control group were markedly increased as compared with the CD group (**Figure 2C**). However, expression of ICAM-1, VCAM-1, and LOX-1 were decreased in the ESJ group. We examined whether lower levels of NF-κB-related pro-inflammatory proteins (IL-1β, TNF-α, COX-2, and iNOS) and cholesterol esterification proteins (ABCA1 and ACAT1) were noted in the ESJ group. Aortic tissues from the ESJ group demonstrated increased expression of the CYP7 family of proteins (CYP7A1 and CYP7B1; cytochrome P450, family 7).

We used human umbilical vein endothelial cells (HUVECs) to investigate the molecular mechanisms of the antiatherogenic effects of ESJ. We examined THP-1 cell adhesion to TNF-α-stimulated HUVECs (10 ng/mL). THP-1 cells adhesions to TNF-α-stimulated HUVECs were dramatically inhibited in a dose-dependent manner in the ESJ group (**Figure 3A**). Protein expression of ICAM-1 and VCAM-1 was examined by immunofluorescent assays (**Figure 3**, panels **B** and **C**) and confirmed with Western blot analysis (**Figure 3D**). The expression of TNF-α-induced VCAM-1 and ICAM-1 was inhibited by >70% in the ESJ group (20 μg/mL dose) compared to that in the control group. Quantitative real-time reverse-transcriptase polymerase chain reaction (RT-PCT) analysis was performed to assess the effects of ESJ on transcriptional levels of adhesion molecules and chemokines. The mRNA expressions of VCAM-1 and ICAM-1 were each reduced significantly (approximately 60%) when treated with 20 μg/mL of the ESJ. Besides, the chemokines CX3CL1 (fractalkine) and CCL5 (RANTES) were significantly reduced in HUVECs in a dose-dependent manner by the addition of ESJ (**Figure 3**, panels **D** and **E**), although CCL2 expression was unaffected.

The HUVECs were exposed to TNF-α for 20 min, and this resulted in a gradual translocation of NF-κB p65 to the nucleus, as shown in **Figure 4A**. However, only partial translocation of NF-κB was observed after 20 min of TNF-α stimulation in ESJ treated cells, and this was confirmed by immunofluorescent analysis with p65 antibody after TNF-α stimulation for 20 min. As shown **Figure 4B**, most inactive NF-κB was present in the cytoplasm of the TNF-α-untreated cells, as evidenced by the diffuse staining seen with primary anti-p65 and secondary Texas Red-conjugated antibodies. Treatment with TNF-α led to nuclear

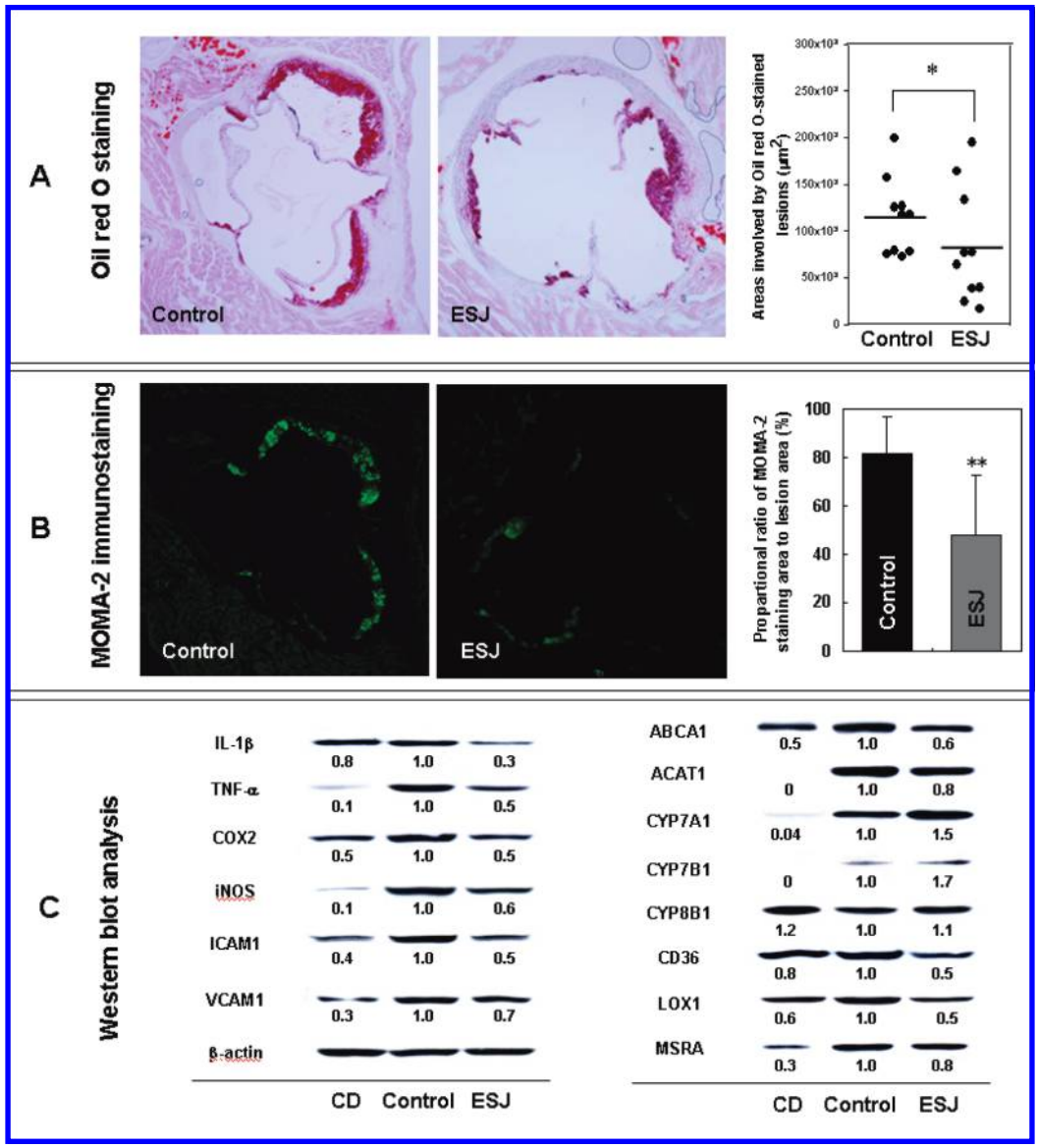

Figure 2. Effects of ESJ on atherosclerotic lesion formation, macrophage accumulation, and protein expression levels in the aortas of LDLR$^{-/-}$ mice. Representative photographs of an aortic valve cross-section (magnification, ×40) from each group are shown. Quantification of oil red O-stained (**A**) and MOMA-2-stained (**B**) aortic valve lesion areas from each group was performed by computer-associated morphometry and is presented in the graph. (**C**) Protein levels were analyzed by Western blot analysis. Results are shown as the mean ± SD, ($n = 10$ in each group). *$p < 0.05$, **$p < 0.01$ vs control group. CD, chow diet-fed group; Control, Western diet-fed group; ESJ, 1% (wt/wt diet) ESJ supplemented Western diet-fed group.

Table 2. Effect of ESJ on Western Diet-Induced Atherosclerotic Lesions in LDLR$^{-/-}$ Mice[a]

	control group ($n = 10$)	ESJ group ($n = 10$)
aortic sinus lesions (distal portion)		
lesion size, $\mu m^2 \times 10^3$	93.8 ± 38.1	71.0 ± 48.6
lesion/whole aortic sinus ratio	17.2 ± 6.7	11.1 ± 6.1*
aortic sinus lesion (proximal portion)		
lesion size, $\mu m^2 \times 10^3$	114.8 ± 41.0	76.9 ± 51.1*
lesion/whole aortic sinus ratio	18.8 ± 4.6	11.9 ± 6.9*
MOMA-2 stain/oil red O stain, %	81.5 ± 15.6	47.5 ± 24.7*

[a] All values are expressed as mean± S.D. *$p < 0.05$ vs control group. Control, western diet-fed group; ESJ, 1% (wt/wt diet) ESJ supplemented western diet-fed group.

localization of fluorescence, which corresponded to intracellular staining with DAPI nuclear dye and emergence of a purple color with cell merging. This suggested that TNF-α induced nuclear localization of NF-κB p65. Bright blue nuclear staining was observed when ESJ pretreated cells were stimulated with TNF-α, and diffuse perinuclear staining of NF-κB p65 was noted. Next, clear IκBα phosphorylation and degradation were observed within 10 min of TNF-α stimulation. However, IκBα phosphorylation and degradation were blocked in the presence of the ESJ (**Figure 4C**), and this suggested that ESJ is specific in inhibiting NF-κB p65 translocation into the nucleus and IκBα proteolysis, in HUVECs. The effects of ESJ on TNF-α-stimulated NF-κB activation in HUVECs was evaluated by EMSA. TNF-α (10 ng/mL) significantly increased the DNA binding activity of NF-κB within 2 h, and pretreatment with ESJ (0 to 20 μg/mL) markedly suppressed this activation (**Figure 4D**).

DISCUSSION

The objective of this study was to investigate the inhibitory effects of ESJ on the development of early atherosclerosis. We examined the expression of adhesion molecules and inflammatory factors in LDLR$^{-/-}$ mice and in TNF-α-stimulated HUVECs.

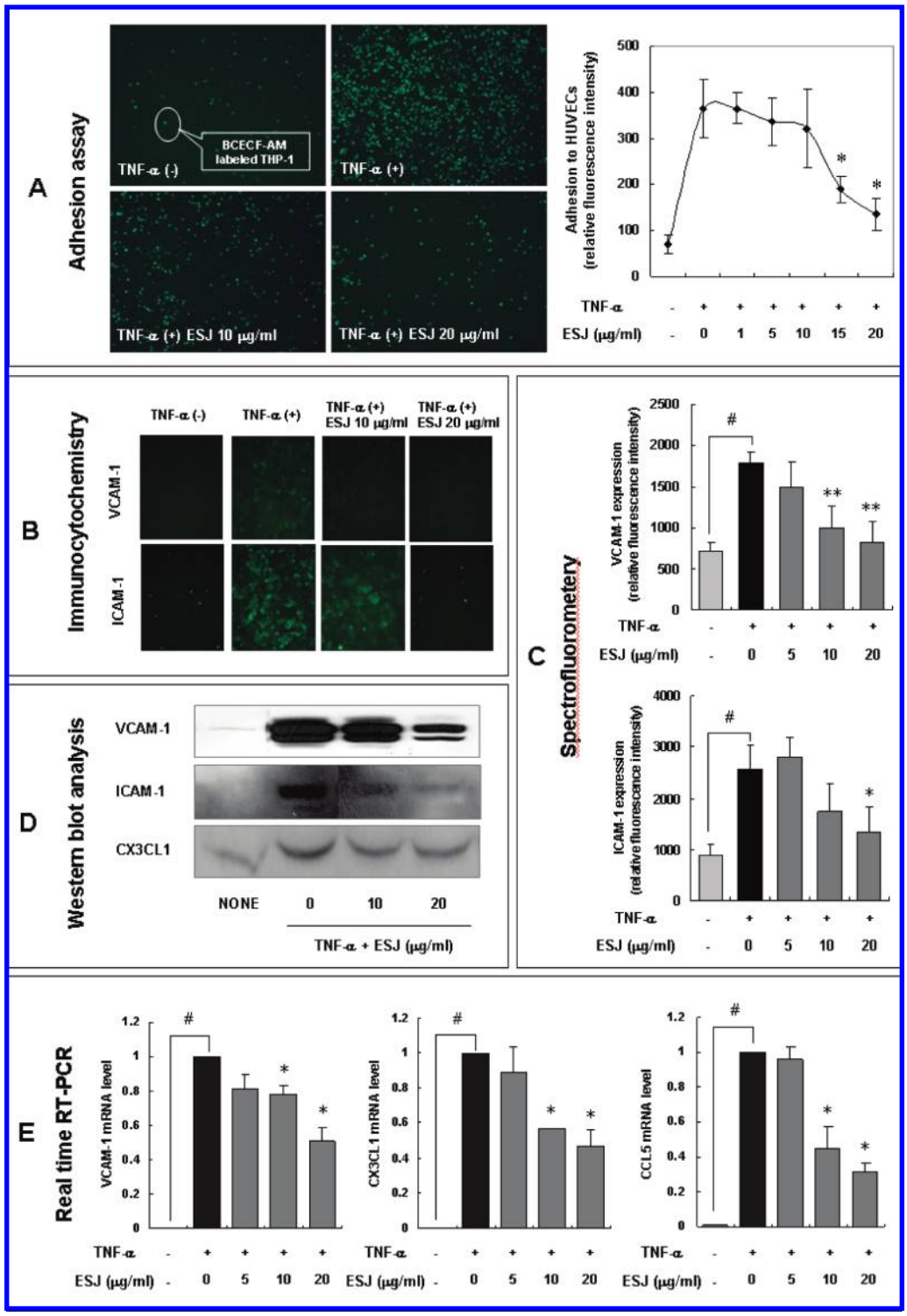

Figure 3. Effects of ESJ on THP-1 monocyte adhesion and expression of adhesion molecules in TNF-α-stimulated HUVECs. (**A**) HUVECs were pretreated with and without ESJ at indicated concentrations for 2 h and then stimulated with 10 ng/mL TNF-α for 6 h. Representative photographs (three independent experiments) were obtained using fluorescence microscopy with a fluorescein blue filter (magnification, ×40). (**B**) Immunocytochemical analysis of adhesion molecule expression in TNF-α-stimulated endothelial cells. VCAM-1 and ICAM-1 expression were obtained with FITC-conjugated antibody fluorescence using fluorescence microscopy (magnification, ×200). (**C**) The bar graphs represent quantitative results against VCAM-1 (upper) and ICAM-1 (below) expression with a spectrofluorometer at 485 nm excitation and 535 nm emission. (**D**) Western blot analysis using antibodies specific for VCAM-1, ICAM-1, and CX3CL1. (**E**) Quantitative RT-PCR analysis on TNF-α-induced expression of adhesion molecules and chemokines. $^{\#}p < 0.01$ vs the media alone-treated group. $^{*}p < 0.05$, $^{**}p < 0.01$ vs TNF-α-alone-treated group.

LDLs are susceptible to lipid peroxidation, resulting in oxidatively modified LDLs, which can inhibit nitric oxide production. Nitric oxide (NO) is a chemical mediator with multiple antiatherogenic properties, including vasorelaxation, and is also involved in the development of atherosclerotic lesions (*3, 4*). The beneficial effects of nutritional antioxidants on the prevention of lipid peroxidation and the reduction of atherosclerotic lesions and overall cardiovascular risk factors are well known (*19, 20*). Common nutritional antioxidants include phenolics and flavonoids, and a fruit-and-vegetable-rich

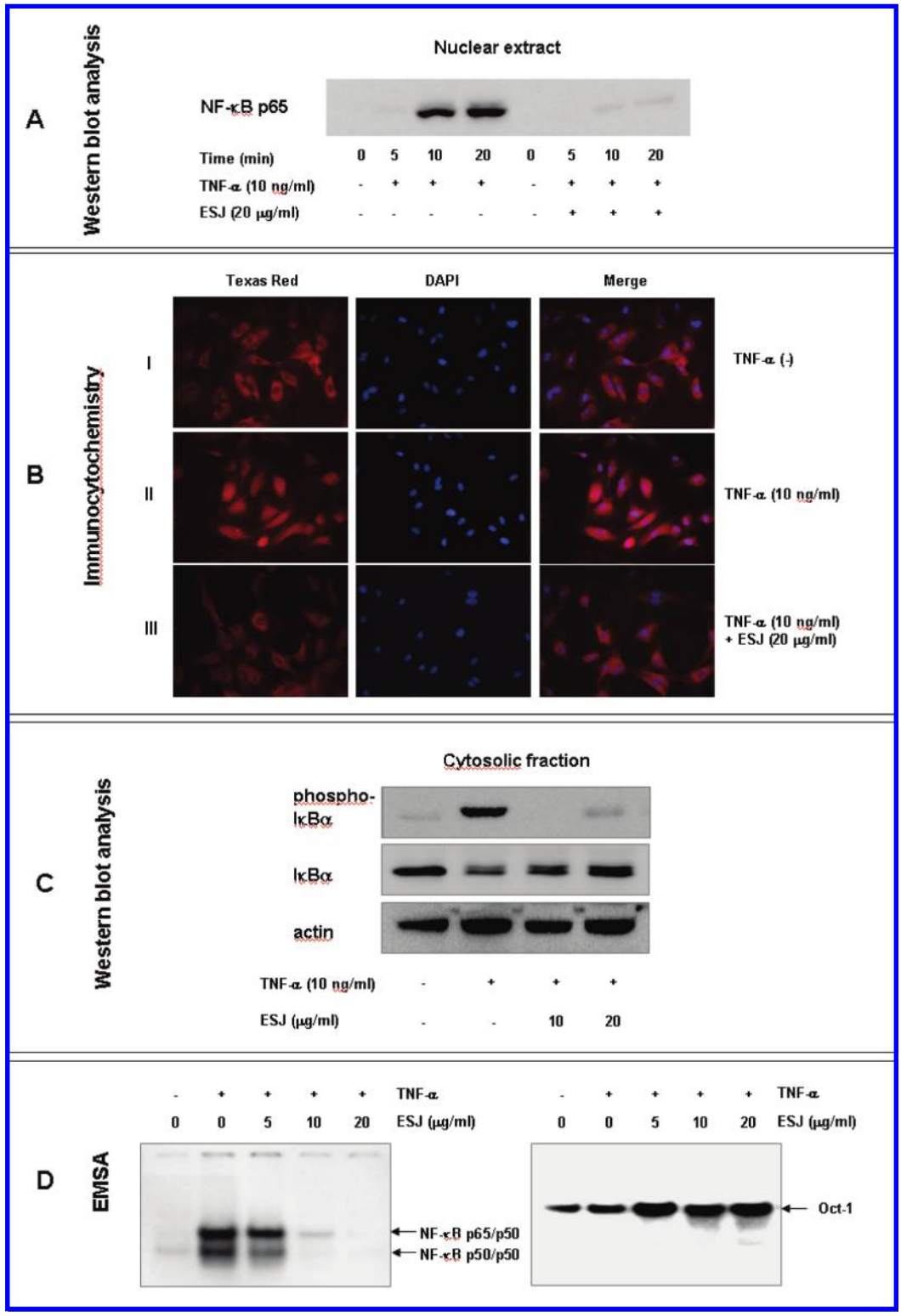

Figure 4. Effects of ESJ on NF-κB activation in TNF-α-stimulated HUVECs. Western blot analysis (**A**) and immunocytochemistry (**B**) for NF-κB localization by using the Texas-red labeled p65 antibody. Cells were either untreated (I), treated with 10 ng/mL TNF-α for 20 min (II), or preincubated with 20 μg/mL ESJ for 2 h, followed by stimulation with TNF-α for 10 min (III). Photomicrographs ($\times$400). HUVECs nuclei stained with DAPI and composite images generated by superimposing photomicrographs are shown in the merge panel. (**C**) Western blot analysis of phosphorylation and degradation of IκBα in the cytoplasmic fractions. HUVECs were cultured with and without ESJ (10 and 20 μg/mL), TNF-α (10 ng/mL), or both for 10 min. The results shown corresponded to representative experiments of three independent assays. (**D**) EMSA analysis of the nuclear extracts was conducted using a ^{32}P-labeled NF-κB and Oct-1 oligonucleotide probe.

diet high in antioxidants may slow the development of cardiovascular diseases (*21*). The ethanolic extract (ESJ) yield from *A. princeps* Pamp. cv. Sajabal was 68.3 g per 2 kg of powdered material. The total phenol and flavonoid contents in the ESJ were 27.78 g gallic acid equivalents/100 and 12.57 g catechin equivalents/100 g, respectively (*12*). And the quantity of eupatilin and jaceosidin, the two major flavonoids in the ESJ, were analyzed by HPLC. ESJ contains 5.98 g eupatilin and

3.06 g jaceosidin per 100 g, respectively (*12*). Pharmacologically active constituents in ESJ include 4 flavonoids (eupatilin, jaceosidin, apigenin, and euapfolin) (*22*) with LDL-antioxidative and antidiabetic activities (*12*, *15*). Our previous studies showed that jaceosidin had potent LDL-antioxidant activity and suppressed the production of reactive oxygen species and NO as well as the expression of TNF-α and IL-6 in lipopolysaccharide-stimulated RAW264.7 cells (*15*). In the present study, we found that ESJ markedly reduced circulating ox-LDL despite hyperlipidemia as control group and simultaneously diminished circulating iNOS, TNF-α, and IL-1β levels in plasma. Our data suggests that ESJ provides a beneficial role in the inhibition of ox-LDL-induced pro-inflammatory processes and exerts positive effects in the prevention of atherosclerosis.

LDL antioxidants have a beneficial role with reduced atherosclerosis progression, and this effect is associated with decreased recruitment of monocytes, macrophages, and T lymphocytes in the vascular wall (*23*). Our results revealed that 34% of macrophage accumulation in the vessel intima was significantly suppressed in the ESJ group, and this is likely due to the decreased expression of aortic atherosclerotic markers including adhesion molecules and scavenger receptors (*24*). Furthermore, VCAM-1 and ICAM-1 expression in aortas from Western diet-fed LDLR$^{-/-}$ mice (control group) was markedly increased as compared to that in the chow diet-fed C57BL/6J mice (CD group). However, the ESJ group showed lower diet-induced ICAM-1 and VCAM-1 expression, and similar results were noted in the endothelial cell model. This suggested that there was decreased monocyte recruitment into the aortic arch subendothelial spaces through inhibition of the expression of these molecules in the ESJ group. The ESJ decreased the expression level of the NF-κB related pro-inflammatory proteins, IL-1β, TNF-α, COX-2, and iNOS, as well as the cholesterol esterification proteins, ABCA1 and ACAT1. The expressions of CYP7 family proteins (CYP7A1, CYP7B1; cytochrome P450, family 7) were increased in aortas of the ESJ group. These proteins are important as enzymes for bile acid formation and cholesterol metabolism (*25*). Such data indicate that ESJ blocked atherosclerosis by down-regulation of adhesion molecules associated with NF-κB activation and up-regulation of CYP7 family proteins, which results in the inhibition of lipid peroxidation and decreased expression of scavenger receptors (CD36 and LOX-1) and adhesion molecules (ICAM-1 and VCAM-1). Therefore, ESJ may provide a beneficial role in the early stages of atherosclerosis.

Chemokines are small cytokines (most being 8−10 kDa) involved in immune responses and are classified into four subfamilies: C, CC, CXC, and CX3C according to the location of the first four conserved cysteine residues (*26*). Monocyte chemoattractant protein-1 (MCP-1/CCL2) is a representative member as an atherogenic chemokine (*27*). Fractalkine (CX3CL1) functions as a chemoattractant factor and pro-inflammatory cytokine by attracting activation and migration of leukocytes to sites of inflammation or tissue injury. It also acts as an adhesion molecule by binding to CX3CR1 expressed on leukocytes (*28*). Studies have suggested that therapeutic interruption of CXCL1 binding to CX3CR1 may be beneficial in the treatment of cardiovascular disease (*29*). Our data revealed that although ESJ did not affect CCL2 expression, it did significantly reduce CX3CL1 (fractalkine) and CCL5 (RANTES) in HUVECs in a dose-dependent manner. This suggests that ESJ could reduce chemokine expression with enough magnitude to prevent the development of atherosclerosis.

Many human diseases including atherosclerosis, diabetes, arthritis, and cardiovascular diseases involve inflammatory processes with the NF-κB signaling pathway in a central role in disease pathogenesis (*30*). Among these diseases is atherosclerosis, where there is evidence of activation of the NF-κB signaling pathway in atherosclerotic lesions (*31*). Inflammatory genes including cytokines, chemokines, adhesion molecules, and growth factors contain functional NF-κB sites in their promoters, and NF-κB activation is essential for the expression of pro-inflammatory genes (*32*). Studies have revealed that ESJ and its flavonoids (jaceosidin and eupatilin) possess inhibitory activity against the expression of pro-inflammatory cytokines and that this inhibitory mechanism may be associated with inhibition of NF-κB activation (*15*, *33*). Furthermore, ESJ attenuates the TNF-α-induced NF-κB p65 translocation into nucleus, and this leads to decreased expression of adhesion molecules, chemokines, and inflammatory cytokines. These results suggest that ESJ had strong antiatherosclerotic activity.

In conclusion, ESJ suppressed circulating ox-LDL levels, which play important roles in the initiation and progression of atherosclerosis. The resulting decreased in inflammatory processes mediated by cytokines and mediators in Western diet-fed LDLR$^{-/-}$ mice. Therefore, ESJ attenuated the diet-induced aortic macrophage infiltration to the aorta and decreased atherosclerotic lesion formation. Furthermore, ESJ displayed antiatherosclerotic activity due to its ability to decrease intracellular NF-κB signaling, and this led to the down-regulation of adhesion molecule and pro-inflammatory cytokine expression by TNF-α.

LITERATURE CITED

(1) Steinberg, D.; Parthasarathy, S.; Carew, T. E.; Khoo, J. C.; Witztum, J. L. Beyond cholesterol modifications of low-density lipoprotein that increase its atherogenicity. *N. Engl. J. Med*. **1989**, *320*, 915–924.

(2) Yla-Herttuala, S.; Palinski, W.; Rosenfeld, M. E.; Parthasarathy, S.; Carew, T. E.; Butler, S.; Witztum, J. L.; Steinberg, D. Evidence for the presence of oxidatively modified low density lipoprotein in atherosclerotic lesions of rabbit and man. *J. Clin. Invest*. **1989**, *84*, 1086–1095.

(3) Steinberg, D. Low density lipoprotein oxidation and its pathobiological significance. *J. Biol. Chem*. **1997**, *272*, 20963–20966.

(4) Ross, R. Atherosclerosis: an inflammatory disease. *N. Engl. J. Med* **1999**, *340*, 115–26.

(5) Lusis, A. J. Atherosclerosis. *Nature* **2000**, *407*, 233–241.

(6) Iademarco, M. F.; McQuillan, J. J.; Rosen, G. D.; Dean, D. C. Characterization of the promoter for vascular cell adhesion molecule-1 (VCAM-1). *J. Biol. Chem*. **1992**, *267*, 16323–16329.

(7) Collins, T.; Read, M. A.; Neish, A. S.; Whitley, M. Z.; Thanos, D.; Maniatis, T. Transcriptional regulation of endothelial cell adhesion molecules: NF-kappa B and cytokine-inducible enhancers. *FASEB J*. **1995**, *9*, 899–909.

(8) O′Sullivan, B.; Thompson, A.; Thomas, R. NF-kappa B as a therapeutic target in autoimmune disease. *Expert Opin. Ther. Targets* **2007**, *11*, 111–22.

(9) Ledebur, H. C.; Parks, T. P. Transcriptional regulation of the intercellular adhesion molecule-1 gene by inflammatory cytokines in human endothelial cells. Essential roles of a variant NF-kappa B site and p65 homodimers. *J. Biol. Chem*. **1995**, *270*, 933–943.

(10) Zhao, Q. C.; Kiyohara, H.; Yamada, H. Anti-complementary neutral polysaccharides from leaves of *Artemisia princeps*. *Phytochemistry* **1994**, *35*, 73–77.

(11) Umano, K.; Hagi, Y.; Nakahara, K.; Shoji, A.; Shibamoto, T. Volatile chemicals identified in extracts from leaves of Japanese mugwort (*Artemisia princeps* pamp.). *J. Agric. Food Chem*. **2000**, *48*, 3463–3469.

(12) Jung, U. J.; Baek, N. I.; Chung, H. G.; Bang, M. H.; Yoo, J. S.; Jeong, T. S.; Lee, K. T.; Kang, Y. J.; Lee, M. K.; Kim, H. J.; Yeo, J. Y.; Choi, M. S. The anti-diabetic effects of ethanol extract from two variants of *Artemisia princeps* Pampanini in C57BL/KsJ-db/db mice. *Food Chem. Toxicol*. **2007**, *45*, 2022–2029.

(13) Lee, S. H.; Shin, Y. W.; Bae, E. A.; Lee, B.; Min, S.; Baek, N. I.; Chung, H. G.; Kim, N. J.; Kim, D. H. Lactic acid bacteria increase antiallergic effect of *Artemisia princeps* pampanini SS-1. *Arch. Pharm. Res*. **2006**, *29*, 752–756.

(14) Ryu, S. N.; Han, S. S.; Yang, J. J.; Jeong, H. G.; Kang, S. S. Variation of eupatilin and jaceosidin content of mugwort. *Korean J. Crop Sci* **2005**, *50* (Suppl), 204–207.

(15) Kim, M. J.; Han, J. M.; Jin, Y. Y.; Baek, N. I.; Bang, M. H.; Chung, H. G.; Choi, M. S.; Lee, K. T.; Sok, D. E.; Jeong, T. S. In vitro antioxidant and anti-inflammatory activities of Jaceosidin from *Artemisia princeps* Pampanini cv. Sajabal. *Arch. Pharm. Res*. **2008**, *31*, 429–437.

(16) Choi, E. J.; Oh, H. M.; Na, B. R.; Ramesh, T. P.; Lee, H. J.; Choi, C. S.; Choi, S. C.; Oh, T. Y.; Choi, S. J.; Chae, J. R.; Kim, S. W.; Jun, C. D. Eupatilin protects gastric epithelial cells from oxidative damage and down-regulates genes responsible for the cellular oxidative stress. *Pharm. Res*. **2008**, *25*, 1355–1364.

(17) Clavin, M.; Gorzalczany, S.; Macho, A.; Munoz, E.; Ferraro, G.; Acevedo, C.; Martino, V. Anti-inflammatory activity of flavonoids from *Eupatorium arnottianum*. *J. Ethnopharmacol*. **2007**, *112*, 585–589.

(18) Han, J. M.; Lee, W. S.; Kim, J. R.; Son, J.; Nam, K. H.; Choi, S. C.; Lim, J. S.; Jeong, T. S. Effects of diarylheptanoids on the tumor necrosis factor-alpha-induced expression of adhesion molecules in human umbilical vein endothelial cells. *J. Agric. Food Chem*. **2007**, *55*, 9457–9464.

(19) Crawford, R. S.; Kirk, E. A.; Rosenfeld, M. E.; LeBoeuf, R. C.; Chait, A. Dietary antioxidants inhibit development of fatty streak lesions in the LDL receptor-deficient mouse. *Arterioscler., Thromb., Vasc. Biol*. **1998**, *18*, 1506–1513.

(20) Hasty, A. H.; Gruen, M. L.; Terry, E. S.; Surmi, B. K.; Atkinson, R. D.; Gao, L.; Morrow, J. D. Effects of vitamin E on oxidative stress and atherosclerosis in an obese hyperlipidemic mouse model. *J. Nutr. Biochem*. **2007**, *18*, 127–133.

(21) Morton, L. W.; Abu-Amsha Caccetta, R.; Puddey, I. B.; Croft, K. D. Chemistry and biological effects of dietary phenolic compounds: relevance to cardiovascular disease. *Clin. Exp. Pharmacol. Physiol*. **2000**, *27*, 152–159.

(22) Bang, M. H.; Kim, D. H.; Yoo, J. S.; Lee, D. Y.; Song, M. C.; Yang, H. J.; Jeong, T. S.; Lee, K. T.; Choi, M. S.; Chung, H. G.; Baek, N. I. Development of biologically active compounds from edible plant sources XIV. Isolation and identification of flavonoids from the aerial parts of Sajabalssuk (*Artemisia herba*). *J. Korean Soc. Appl. Biol. Chem* **2005**, *48*, 418–420.

(23) Hayek, T.; Fuhrman, B.; Vaya, J.; Rosenblat, M.; Belinky, P.; Coleman, R.; Elis, A.; Aviram, M. Reduced progression of atherosclerosis in apolipoprotein E-deficient mice following consumption of red wine, or its polyphenols quercetin or catechin, is associated with reduced susceptibility of LDL to oxidation and aggregation. *Arterioscler., Thromb., Vasc. Biol*. **1997**, *17*, 2744–2752.

(24) Febbraio, M.; Podrez, E. A.; Smith, J. D.; Hajjar, D. P.; Hazen, S. L.; Hoff, H. F.; Sharma, K.; Silverstein, R. L. Targeted disruption of the class B scavenger receptor CD36 protects against atherosclerotic lesion development in mice. *J. Clin. Invest*. **2000**, *105*, 1049–1056.

(25) Li, Y. C.; Wang, D. P.; Chiang, J. Y. Regulation of cholesterol 7 alpha-hydroxylase in the liver. Cloning, sequencing, and regulation of cholesterol 7 alpha-hydroxylase mRNA. *J. Biol. Chem*. **1990**, *265*, 12012–12019.

(26) Reape, T. J.; Groot, P. H. Chemokines and atherosclerosis. *Atherosclerosis* **1999**, *147*, 213–225.

(27) Terkeltaub, R.; Boisvert, W. A.; Curtiss, L. K. Chemokines and atherosclerosis. *Curr. Opin. Lipidol*. **1998**, *9*, 397–405.

(28) Bazan, J. F.; Bacon, K. B.; Hardiman, G.; Wang, W.; Soo, K.; Rossi, D.; Greaves, D. R.; Zlotnik, A.; Schall, T. J. A new class of membrane-bound chemokine with a CX3C motif. *Nature* **1997**, *385*, 640–644.

(29) Lesnik, P.; Haskell, C. A.; Charo, I. F. Decreased atherosclerosis in CX3CR1−/−mice reveals a role for fractalkine in atherogenesis. *J. Clin. Invest*. **2003**, *111*, 333–340.

(30) Chung, H. Y.; Sung, B.; Jung, K. J.; Zou, Y.; Yu, B. P. The molecular inflammatory process in aging. *Antioxid. Redox. Signaling* **2006**, *8*, 572–581.

(31) Hajra, L.; Evans, A. I.; Chen, M.; Hyduk, S. J.; Collins, T.; Cybulsky, M. I. The NF-kappa B signal transduction pathway in aortic endothelial cells is primed for activation in regions predisposed to atherosclerotic lesion formation. *Proc. Natl. Acad. Sci. U.S.A*. **2000**, *97*, 9052–9057.

(32) Read, M. A.; Whitley, M. Z.; Williams, A. J.; Collins, T. NF-kappa B and I kappa B alpha: an inducible regulatory system in endothelial activation. *J. Exp. Med* **1994**, *179*, 503–512.

(33) Lee, S. H.; Bae, E. A.; Park, E. K.; Shin, Y. W.; Baek, N. I.; Han, E. J.; Chung, H. G.; Kim, D. H. Inhibitory effect of eupatilin and jaceosidin isolated from *Artemisia princeps* in IgE-induced hypersensitivity. *Int. Immunopharmacol*. **2007**, *7*, 1678–1684.

Received for review August 27, 2008. Revised manuscript received November 9, 2008. Accepted November 24, 2008. This work was supported by a grant from the Ganghwa County Agricultural Technology Center for "Evaluation of biological activity and pharmacological efficacy for plants indigenous to Ganghwa".

JF802639Y